Published in final edited form as:
Invest Ophthalmol Vis Sci. 2009 June ; 50(6): 2919–2926. doi:10.1167/iovs.08-3070.

Mechanism of Cataract Formation in αA-crystallin Y118D Mutation

Qingling Huang[1], **Linlin Ding**[1], **Kim B. Phan**[1], **Catherine Cheng**[2,3], **Chun-hong Xia**[2], **Xiaohua Gong**[2,3], and **Joseph Horwitz**[1]

[1] Jules Stein Eye Institute, University of California Los Angeles, Los Angeles, California

[2] School of Optometry and Vision Science Program, University of California Los Angeles, Los Angeles, California

[3] UC Berkeley/UCSF Joint Bioengineering Graduate Program, University of California Berkeley, Berkeley, California.

Abstract

Purpose—The aim of this study was to elucidate the molecular mechanisms that lead to a dominant nuclear cataract in a mouse harboring the Y118D mutation in the αA-crystallin gene.

Methods—The physicochemical properties of α-crystallin obtained from mouse lenses with the Y118D mutation as well as a recombinant Y118D αA-crystallin were studied using gel filtration, two-dimensional (2D) gel electrophoresis, multi-angle light scattering, circular dichroism, fluorescence, and chaperone activities.

Results—Both native α-crystallin from mutant lens and recombinant αA-Y118D displayed higher molecular mass distribution than the wild-type. Circular dichroism spectra indicated changes in the secondary structures of αA-Y118D. The αA-Y118D protein prevented nonspecific protein aggregation more effectively than wild-type αA-crystallin. The gel filtration and 2D gel electrophoresis analysis showed a significant reduction of Y118D mutant protein in comparison with wild-type αA protein of heterozygous mutant lenses. Quantitative RT-PCR results confirmed a decrease in αA and αB transcripts in the homozygous mutant α A(Y118D/Y118D) lenses.

Conclusions—The αA-Y118D mutant protein itself displays an increased chaperone-like activity. However, the dominant nuclear cataract is associated with a significant decrease in the amount of αA-crystallin, leading to a reduction in total chaperone capacity needed for maintaining lens transparency.

Alpha-crystallin is the major protein of vertebrate eye lens, and plays a structural role in maintaining the lens transparency and proper refractive index. It is composed of two highly homologous subunits, αA and αB.[1,2] Although the molecular weight of each individual subunit is approximately 20 kDa, the α-crystallins exist as multimers, with mass ranging from ~300 to more than 1000 kDa. The size of the oligomer varies depending on the temperature, pH, and ionic strength.[3] The two subunits assemble in vivo to form heteromeric oligomers by means of subunit exchange.[4,5]

Corresponding author: Joseph Horwitz, B-168, Jules Stein Eye Institute, 100 Stein Plaza, University of California Los Angeles, Los Angeles, CA 90095; horwitz@jsei.ucla.edu..

Disclosure: **Q. Huang**, None; **L. Ding**, None; **K.B. Phan**, None; **C. Cheng**, None; **C. Xia**, None; **X. Gong**, None; **J. Horwitz**, None

Both αA- and αB-crystallins are members of the small heat shock protein (sHSP) family.[6] αA is primarily expressed in the lens, and low amounts are found in retina and many other non-ocular tissues, including spleen and thymus.[7,8] Unlike αA-crystallin, αB-crystallin is stress inducible and is also found in the heart, muscle, and brain.[9–11] Ubiquitous expression of αB signifies cell protection against various stresses such as thermal,[12,13] hypertonic,[14] oxidative insults,[15] and apoptosis.[16] As a molecular chaperone, α-crystallin binds to misfolded proteins and suppresses their nonspecific aggregation.[17,18] This function is very important for the lens in preventing cataract, as proteins are subjected to various stresses over the lifetime of the organism and are highly susceptible to denaturation and aggregation. In the lens, α-crystallin binds to various lens abundant proteins such as the β- and γ-crystallins[2] as well as other housekeeping enzymes.[19] α-Crystallin was also shown to interact with intermediate filaments[20,21] and inhibit cytochalasin-induced depolymerization of actin,[22] suggesting it plays an important role in maintaining the integrity of cytoskeleton.

Genetic and biochemical studies suggest that some forms of lens opacities or cataracts are associated with decreased chaperone-like activities of α-crystallins. The αA(−/−) knockout mice develop microphthalmia and small lenses with nuclear cataracts.[23] The nuclear cataract is associated with αB inclusion bodies and a significant amount of water insoluble γ-crystallin.[2] Unexpectedly, the αB(−/−) knockout mice develop clear lenses,[24] in addition, lens epithelial cells derived from αB-crystallin knockout mice undergo hyperproliferation[25] in culture. Mutations of either αA- or αB-crystallin cause dominant or recessive cataracts in humans and mice. The human αA-R49C, αA-R116C, and αA-R116H missense mutations and the mouse αA-V124E missense mutation are linked to dominant nuclear cataracts.[26–29] Human αA-W9X nonsense mutation and human αA-R54C point mutations, as well as mouse αA-R54H or R54C mutations, cause recessive cataracts.[30–33] A frame-shift mutation and a missense mutation αB-R120G cause dominant cataracts in humans.[34] The Arg^{116} of αA-crystallin is the residue corresponding to the Arg^{120} of αB-crystallin, and both αA-R116C and αB-R120G mutant proteins have decreased chaperone-like activities for some target proteins in vitro.[35–37] Transgenic mice that express human αA-R116C reveal unique pathologic events.[38] Recently, the human αB-D140N mutation has been shown to cause dominant cataracts by abolishing its chaperone-like activity and by acting as a dominant negative inhibitor to suppress the chaperone-like activity of wild-type αB-crystallin.[39] Thus, it is clear that a decreased chaperone-like activity of α-crystallin is detrimental to the lens transparency. However, it is unclear whether an increased chaperone-like activity of α-crystallin is beneficial for the lens transparency.

In our previous study,[33] we reported that a dominant nuclear cataract, identified from ENU-induced mouse mutations, was caused by αA-Y118D point mutation. This cataract was associated with increased water-insoluble crystallins including α-, β-, and γ-isoforms in the lens. However, the mechanism for how αA-Y118D mutation reduces the solubility of other lens proteins is unknown. Here we present new mechanistic information for nuclear cataract formation in the αA-Y118D mutation. This mutation causes a major decrease in the amount of α-crystallin available for chaperone protection, thereby destabilizing the lens.

Materials and Methods

Recombinant bovine wild-type αA-crystallin was expressed and purified as previously described.[40] Tris(2-carboxyethyl)phosphine (TCEP) was purchased from Pierce Biotechnology (Rockford, IL). Insulin and ovotransferrin were obtained from Sigma (St. Louis, MO). Buffer A contained 100 mM NaCl and 50 mM $NaPO_4$ (pH 7.0).

Preparation of Water-Soluble and Water-Insoluble Lens Protein Fractions

Lenses were homogenized in buffer A at a ratio of 200 μL per 5 mg of lens wet-weight. The homogenate was then centrifuged at 18,000*g* for 15 minutes at 4°C. The supernatant was used as the water-soluble fraction. The pellet was re-homogenized with buffer A and centrifuged at 18,000*g* for 15 minutes. The supernatant was discarded. This procedure was repeated three times and the final pellet was used as the water-insoluble fraction.

Making the αA-Y118D cDNA Construct

The cDNA construct of bovine αA-Y118D mutant was prepared by overlap extension using two rounds of PCR with appropriate primers.[41] The correct construct was confirmed by DNA sequencing.

Expression and Purification of αA-crystallin Y118D Mutant Protein

Expression and purification of αA-Y118D protein was carried out as previously described.[40] Protein concentration of αA was determined from absorbance at 280 nm using extinction coefficient 13,000 M^{-1} cm^{-1}.[42]

Molar Mass Determination

The molar mass (M_r) distribution of αA-Y118D was determined by size exclusion chromatography (AKTA Basic System; GE Healthcare, Piscataway, NJ) using a column (Superose 6 HR10/30; GE Healthcare) coupled online with a UV-900 detector, a multi-angle laser light scattering detector (Down-EOS Wyatt Technology, Santa Barbra, CA), and a refractive index detector (Optilab-DSP; Wyatt Technology).[2,43–45]

Circular Dichroism Measurements

Far UV and near UV circular dichroism (CD) measurements were performed using a spectropolarimeter (Jasco J-810; Jasco, Inc., Easton, MD). Temperature was controlled with Peltier type temperature control system (Model PTC-348WI; Jasco). Protein samples were prepared in buffer containing 50 mM $NaPO_4$ and 33.33 mM Na_2SO_4 (pH 7.2). Estimation of secondary structure parameters was performed using CDPro program CONTIN method with an expanded reference set.[46,47]

Assays for Chaperone-like Activity

Aggregation assay was carried out as described previously.[48] Insulin and ovotransferrin were unfolded at 37°C by cleavage of the disulfide bonds with TCEP.

Two-Dimensional Gel Electrophoresis

Two-dimensional gel electrophoresis was performed as previously described.[33]

Quantitative RT-PCR

Total RNA samples were prepared from the lenses of 3 weeks old mice by using an isolation reagent (TRIzol Reagent; Gibco, Grand Island, NY) with standard procedures. First-strand cDNA synthesis was performed by RT-PCR (SuperScript RT-PCR; Invitrogen, Carlsbad, CA). Quantitative PCR was performed using a SYBR-green kit and a real-time PCR system (ABI Prism 7000 Sequence Detection System; Applied Biosystems, Foster City, CA), with primers for 18S rRNA, αA-, and αB-crystallin (18S rRNA: antisense 5′-CATTCTTGGCAAATGC TTTCG-3′, sense 5′-GCCGCTAGAGGTGAAATTCTTG-3′; αA: antisense 5′-TTTGTCATCTTCTTGGACGTGAA-3′, sense 5′-ATGGTCATCCTGCCTCTCGTT-3′; αB: antisense 5′-CGGAGGAACTCAAAGTCAAGGTT-3′, sense 5′-TGTTCGTCCTGGCGTTCTTC-3′).

Results

Distribution of Lens Water-Soluble Proteins in αA-Y118D Mutant

Figure 1 shows the water-soluble protein distribution of the mutant αA-Y118D lens compared to the wild-type lens. As was reported previously, the αA(Y118D/Y118D) homozygous lens weighs approximately 19% less than the wild-type lens.[33] Thus, for a meaningful comparison between the wild-type and the homozygous lenses, we have compared the protein amount per equal lens volume. It is evident that the amount of water-soluble protein in the same unit volume of the homozygous mutant lens is significantly less than the wild-type lens. Integrating the total area under the chromatogram, we find that the mutant has 37% less total soluble proteins than the wild-type. Of particular interest is the relative loss of α-crystallin and the significant increase in the void volume peak. A two-dimensional gel electrophoresis of the void volume peak material in the mutant lens shows that it is composed of the various α-crystallin polypeptides and significant amounts of γ-crystallin.

Molecular Weight Distribution of Native Total α-crystallin from αA(Y118D/Y118D) Lenses, and Recombinant Y118D αA-crystallin

As shown in Figure 1, the α-crystallin from the mutant lens appears as a broad band eluting approximately between 9 mL and 13 mL. This fraction was collected and then subjected to molecular weight distribution by light scattering. Figure 2A shows the molar mass distribution of the Y118D α-crystallin compared with the wild-type α-crystallin. The molar mass at the peak of the mutant is 1.4×10^6 daltons, whereas the peak of the wild-type α-crystallin is 8.6×10^5 daltons. Similar to the known properties of wild-type α-crystallin, the mutant α-crystallin is highly heterogeneous.

The data presented in Figure 2A is from total α-crystallin, consisting of αA and αB at an approximate molar ratio of 2 αA to 1 αB. To study the properties of purified αA-Y118D crystallin, a recombinant protein was prepared as described in above. Figure 2B shows the molar mass distribution of recombinant αA-Y118D with a peak of 1.2×10^6 daltons, compared with recombinant wild-type αA-crystallin with a peak of 5×10^5 daltons.

Effects of Temperature on the Oligomeric State of αA-Y118D Protein

When wild-type αA-crystallin is heated from 25°C to 37°C, there is no significant change in its molecular weight distribution; it is essentially the same as shown in Figure 2B at 25°C. On heating to 45°C higher oligomers are formed with the peak at 6×10^5 daltons (data not shown). In comparison, αA-Y118D is more sensitive to temperature changes. On changing the temperature from 25°C to 37°C, the molar mass at the peak increases from 1.2×10^6 daltons to 1.5×10^6 daltons. Further increase in the temperature to 45°C results in a shift of the peak molar mass to 2.2×10^6 daltons (Fig. 2B). Since the molecular mass of monomeric αA-crystallin is approximately 20,000 daltons, it implies that at 37°C the mutant oligomer at the peak elution is made up of an average of 75 subunits, whereas wild-type αA-crystallin under this condition is made up of approximately 25 subunits.

Secondary and Tertiary Structure of Recombinant αA-Y118D Protein

The far ultraviolet circular dichroism (CD) spectra of αA-Y118D crystallin and wild-type αA-crystallin are shown in Figure 3A. The intensity of the negative band at 215 nm for the mutant protein is significantly stronger than that of the wild-type αA. A complete analysis of the CD spectra using three different methodologies is given in Table 1. The most consistent difference seen is the increase in α-helical structure of the mutant protein. Results are also presented in Table 1 from the data accumulated at 45°C. A consistent result is that raising the temperature increases the percent α helix of the protein.

The near ultraviolet spectra of αA-Y118D and wild-type αA are shown in Figure 3B. The well-defined vibronic peak at 292 nm can be positively assigned to the ^1L_b band of the single tryptophan residue W9.[49,50] Interestingly, in the αA-Y118D mutant, the intensity of the ^1L_b band is greatly diminished. This means that the mutation caused the tryptophan environment to change. It is impossible at this stage to pinpoint the exact changes in the tertiary structure. The tryptophan fluorescence spectra of the wild-type αA and the αA-Y118D mutant are shown in Figure 4. Both proteins exhibit an emission maximum at 334 nm on excitation at 295 nm, suggesting a buried environment for this tryptophan. The tyrosine mutation caused the tryptophan spectra to be less quenched than the wild-type.

Comparing the Chaperone-like Activity of αA-Y118D with Wild-Type αA

The chaperone-like activity of αA-crystallin was examined by its ability to control the aggregation of the two target-proteins insulin and ovotransferrin. Both of these proteins can be unfolded by reduction of their disulfide bands with TCEP, as shown in Figures 5A and 5B. The mutant Y118D was much more effective in lowering the scattering due to aggregation than the wild-type αA. Similar results were obtained when we used α-lactalbumin as a target protein (data not shown).

The ability of α-crystallin to suppress aggregation was also tested on total soluble lens homogenate of a mutant αA(Y118D/Y118D) homozygote and a wild-type lens soluble homogenate. As shown in Figure 6, on heating to 60°C for 2 hours, the total soluble protein from the wild-type lens did not exhibiting significant scattering (curve 1). On the other hand, the total soluble protein from the mutant lens aggregate very fast (curve 2). As was shown in Figure 1, the total amount of α-crystallin in the mutant lens is significantly lower than in the wild-type lens. If we add exogenous recombinant αA-Y118D, it can suppress the aggregation of the total soluble mixture (curve 3). This experiment implies that there is not enough αA-crystallin available in the mutant lens.

To confirm that the total amount of α-crystallin in the αA(Y118D/Y118D) mutant is significantly less than in the wild-type lenses, we selected the heterozygous αA(Y118D/+) lenses for a comparison between the wild-type αA-crystallin and the αA-Y118D mutant. The Y118D mutation with an extra negative residue in the protein allows for a clear separation between wild-type and the mutant proteins on a 2D gel analysis, shown in Figure 7. Water-soluble and water-insoluble samples were prepared from the same lenses. Based on the densitometry measurements of the protein spots in the 2D gels, αA-Y118D was 50% less in concentration than the wild-type αA in the water-soluble fraction. For the water-insoluble fraction, the densitometry showed that the αA Y118D amount was 35% less than the wild-type (Fig. 7). In agreement to the data, shown in Figure 7, a quantitative comparison of wild-type and αA-Y118D homozygous lenses on a 2D gel also revealed that total αA-crystallin in the mutant was significantly less than in the wild-type. Moreover, quantitative RT-PCR measurements indicated that αA and αB mRNA transcripts in homozygous mutant lenses were reduced by 30% when compared to transcripts in wild-type lenses (Fig. 8). The fact that αB transcripts were also reduced may suggest a general RNA and protein degradation as secondary consequence of this mutation.

Discussion

This work supports the notion that lens transparency relies on the sufficient amount of αA-crystallin with the appropriate quaternary structure and chaperone-like activity. The nuclear cataract caused by the αA-Y118D mutation is associated with a significant decrease in the amount of the expressed αA-crystallin, while the chaperone-like properties of the mutated protein are increased.

All sHSPs, including α-crystallins, share a relatively conserved region, the α-crystallin domain, which is a stretch of 80 to 100 amino acid residues at the C-terminal part of the protein. Studies from site-directed spin-labeling identified residues 110 to 113 of αA-crystallin in this conserved region to be involved in inter-subunit interaction.[51] This putative subunit interface lies in a β strand (residues Tyr^{109} through Leu^{120}), which interacts with the equivalent strand of an adjacent subunit in an anti-parallel fashion.[52] The Tyr^{118} residue of αA-crystallin was shown to exist in a buried environment along this beta strand. Tyrosine was reported to have a high propensity in forming beta sheet, but aspartate is among the worst beta sheet-forming residues.[53] Tyrosine 118 is a highly conserved residue among the members of the small heat-shock protein family.[54] The far UV CD data shows that substitution of a tyrosine with an aspartate at residue 118 changed the secondary structure and produced higher order structure of αA-crystallin. Here we show a drastic increase in the molecular weight and changes in the secondary structure with increasing temperature (Fig. 2 and Table 1). Furthermore, αA-Y118D mutation also perturbs the tertiary structure of αA-crystallin as the near UV CD spectra showed altered local environments of the single tryptophan residue (W9).

It is important to note that mutations in the beta strands of the conserved α-crystallin domains (residues 83 to 120) are known to cause autosomal dominant cataract. At present, known human mutations in αA in this region include G98R, R116C, and R116H.[55] All the above-mentioned mutations, including the mouse Y118D, share common physical-chemical properties. The site-directed spin labeling studies show that all the even-numbered residues exist in a buried environment along the β-strand. Interestingly, the known mutations of the even-numbered residues cause a significant increase in the size of αA-crystallin.[51] In addition, the three mutations discussed above are also more sensitive to temperature change. The near UV data of αA- Y118D (Fig. 3B) shows the specific reduction in the intensity of the ^1L_b vibronic transition emanating from the single tryptophan residue W9. Interestingly, similar changes in the near UV CD spectra are obtained for αA-G98R and αA-R116C.[56,57] While much is known in human about the structure of the alpha-crystallin domain from the crystallographic data of Mj16.5, HSP16.9, and TSP 36, as well as from the extensive site-directed spin labeling studies, very little is known about the structure of the N terminus of α-crystallin. Already in 1979, it was shown by limited proteolysis studies that the N terminus is buried and not accessible.[58] The near UV data shows that the mutations G98R, R116C, and Y118D all affect the tryptophan environment at the N terminus. However, the fluorescence data for αA-Y118D (Fig. 4) shows that the tryptophan residue is still in a relative buried environment because the fluorescent emission maxima at 334 is the same as in the wild-type αA.

Earlier work on the chaperone-like properties of R116C mutation suggested a tenfold increase over wild-type in the membrane-binding capacity of the mutant.[36] More recently, Koteiche and Mchaourab[59] showed a definite gain of function of the R116C mutant that leads to a significant increase in its capacity of binding undamaged proteins and ultimately precipitating when the α-crystallin complexes are saturated. The same gain of function is seen with the αA-Y118D mutant being a better chaperone when tested with target proteins such as insulin, α-lactalbumin, and ovotransferrin (Fig. 5). The increased chaperone activity can be due to the exposure of new sites in the mutant protein, or the conversion of low affinity “target” protein binding sites into high affinity sites. Additional kinetic studies will be needed to answer these questions. Based on recent work involving the αA-R116C mutation we suggest that the mutation of αA-Y118D also resulted in the conversion of the low affinity sites into higher affinity binding sites.[59] In the homozygous mutant lenses there is also a significant increase in the binding of α-crystallin to the β- and γ-crystallins. This is evident in the 2D gel of the void volume high-molecular-weight peak shown in the Figure 1 (insert). Analysis of the same fraction obtained from wild-type lenses yields mostly α-

crystallin polypeptides with no significant amount of β- and γ-crystallins (data not shown). One of the major problems with αA-Y118D mutant lenses seems to be the low level of αA-Y118D. Our data show a decrease in the mRNA level in homozygous mutant lenses when compared to the wild-type control. The 2D gel data of the lens water-soluble and water-insoluble protein samples clearly demonstrate that the αA-Y118D mutant protein level is lower than wild-type αA-crystallin level in the heterozygous lenses. However, we cannot conclude that the lower transcriptional level is responsible for the low protein expression. We have noted increases of both phosphorylated and cleaved forms of αA-Y118D mutant proteins in homozygous mutant lenses.[33] Moreover, the yield of the αA-Y118D recombinant proteins is consistently about one-half of the wild-type recombinant proteins in the same recombinant bacterial system (data not shown). This would suggest that the post-translational machinery rather than the transcriptional regulation is probably responsible for the insufficient amount of αA-Y118D mutant proteins in the mutant lenses. Future studies will be needed to conclude if the reduction of the mutant protein results from transcriptional controls, translational controls, or both.

It is known that in the wild-type mammalian lenses there is enough a-crystallin to suppress nonspecific aggregation when the total soluble proteins are heat denatured.[17] This is not the case with the αA-Y118D mutant lenses. As is evident from Figure 6, when wild-type total soluble lens proteins are heated to 60°C, the solution does not scatter. On the other hand, the total lens soluble proteins from the mutant lens aggregates and scatters very rapidly (Figure, curve 2). Adding exogenous recombinant αA-Y118D suppresses the scattering; thus, proving that there is not enough αA in the mutant lens, and that the total chaperone capacity of the mutant lens was reduced. α-Crystallin is recognized as being a multifunctional protein.[7–22] Therefore, the significant reduction in the amount of α-crystallin in the mutant lenses may destabilize the lens in addition to the loss of the total chaperone capacity.

It is reasonable to suggest that the same mechanism that leads to cataract formation in the mouse αA-Y118D mutation is responsible for the cataracts present in the human mutations G98R, R116C, and R116H. These mutations are in close proximity to one another and are on critical beta sheet stretch that is involved in inter-subunit interactions. The physicochemical properties of the recombinant proteins produced of the human mutations are very similar to that obtained from the Y118D mutation. In addition, patients with these mutations develop very similar lens phenotypes. Because the new technologies that are used at present for cataract surgery completely destroy the lenses, it is very unlikely that one will be able to obtain an intact human lens from patients with any of the above-mentioned mutations. Our data strongly suggest that the mouse αA-Y118D mutation is a viable model for the human condition.

Acknowledgments

Supported by National Eye Institute, National Institutes of Health Grants EY03897 and EY013849.

References

1. Bloemendal H, de Jong W, Jaenicke R, Lubsen NH, Slingsby C, Tardieu A. Ageing and vision: structure, stability and function of lens crystallins. Prog Biophys Mol Biol 2004;86:407–485. [PubMed: 15302206]
2. Horwitz J. Alpha-crystallin. Exp Eye Res 2003;76:145–153. [PubMed: 12565801]
3. Siezen RJ, Bindels JG, Hoenders HJ. The quaternary structure of bovine alpha-crystallin. Effects of variation in alkaline pH, ionic strength, temperature and calcium ion concentration. Eur J Biochem 1980;111:435–444. [PubMed: 7460906]

4. van den Oetelaar PJ, van Someren PF, Thomson JA, Siezen RJ, Hoenders HJ. A dynamic quaternary structure of bovine alpha-crystallin as indicated from intermolecular exchange of subunits. Biochemistry 1990;29:3488–3493. [PubMed: 2354148]
5. Bova MP, Ding LL, Horwitz J, Fung BK. Subunit exchange of αA-crystallin. J Biol Chem 1997;272:29511–29517. [PubMed: 9368012]
6. Klemenz R, Frohli E, Steiger RH, Schafer R, Aoyama A. Alpha B-crystallin is a small heat shock protein. Proc Natl Acad Sci USA 1991;88:3652–3656. [PubMed: 2023914]
7. Kato K, Shinohara H, Kurobe N, Goto S, Inaguma Y, Ohshima K. Immunoreactive alpha A crystallin in rat non-lenticular tissues detected with a sensitive immunoassay method. Biochim Biophys Acta 1991;1080:173–180. [PubMed: 1932094]
8. Srinivasan AN, Nagineni CN, Bhat SP. Alpha A-crystallin is expressed in non-ocular tissues. J Biol Chem 1992;267:23337–23341. [PubMed: 1429679]
9. Atomi Y, Yamada S, Strohman R, Nonomura Y. Alpha B-crystallin in skeletal muscle: purification and localization. J Biochem 1991;110:812–822. [PubMed: 1783614]
10. Bhat SP, Nagineni CN. Alpha B subunit of lens-specific protein alpha-crystallin is present in other ocular and non-ocular tissues. Biochem Biophys Res Commun 1989;158:319–325. [PubMed: 2912453]
11. Iwaki T, Kume-Iwaki A, Goldman JE. Cellular distribution of alpha B-crystallin in non-lenticular tissues. J Histochem Cytochem 1990;38:31–39. [PubMed: 2294148]
12. Aoyama A, Frohli E, Schafer R, Klemenz R. Alpha B-crystallin expression in mouse NIH 3T3 fibroblasts: glucocorticoid responsiveness and involvement in thermal protection. Mol Cell Biol 1993;13:1824–1835. [PubMed: 8441415]
13. van den IPR, Overkamp P, Knauf U, Gaestel M, de Jong WW. Alpha A-crystallin confers cellular thermoresistance. FEBS Lett 1994;355:54–56. [PubMed: 7957962]
14. Dasgupta S, Hohman TC, Carper D. Hypertonic stress induces alpha B-crystallin expression. Exp Eye Res 1992;54:461–470. [PubMed: 1381680]
15. Mehlen P, Preville X, Chareyron P, Briolay J, Klemenz R, Arrigo AP. Constitutive expression of human hsp27, Drosophila hsp27, or human alpha B-crystallin confers resistance to TNF- and oxidative stress-induced cytotoxicity in stably transfected murine L929 fibroblasts. J Immunol 1995;154:363–374. [PubMed: 7995955]
16. Mehlen P, Schulze-Osthoff K, Arrigo AP. Small stress proteins as novel regulators of apoptosis. Heat shock protein 27 blocks Fas/APO-1- and staurosporine-induced cell death. J Biol Chem 1996;271:16510–16514. [PubMed: 8663291]
17. Horwitz J. Alpha-crystallin can function as a molecular chaperone. Proc Natl Acad Sci USA 1992;89:10449–10453. [PubMed: 1438232]
18. Muchowski PJ, Bassuk JA, Lubsen NH, Clark JI. Human alphaB-crystallin. Small heat shock protein and molecular chaperone. J Biol Chem 1997;272:2578–2582. [PubMed: 8999975]
19. Velasco PT, Lukas TJ, Murthy SN, Duglas-Tabor Y, Garland DL, Lorand L. Hierarchy of lens proteins requiring protection against heat-induced precipitation by the alpha crystallin chaperone. Exp Eye Res 1997;65:497–505. [PubMed: 9464183]
20. Nicholl ID, Quinlan RA. Chaperone activity of alpha-crystallins modulates intermediate filament assembly. EMBO J 1994;13:945–953. [PubMed: 7906647]
21. Muchowski PJ, Valdez MM, Clark JI. AlphaB-crystallin selectively targets intermediate filament proteins during thermal stress. Invest Ophthalmol Vis Sci 1999;40:951–958. [PubMed: 10102292]
22. Wang K, Spector A. Alpha-crystallin stabilizes actin filaments and prevents cytochalasin-induced depolymerization in a phosphorylation-dependent manner. Eur J Biochem 1996;242:56–66. [PubMed: 8954153]
23. Brady JP, Garland D, Duglas-Tabor Y, Robison WG Jr, Groome A, Wawrousek EF. Targeted disruption of the mouse alpha A-crystallin gene induces cataract and cytoplasmic inclusion bodies containing the small heat shock protein alpha B-crystallin. Proc Natl Acad Sci USA 1997;94:884–889. [PubMed: 9023351]
24. Brady JP, Garland DL, Green DE, Tamm ER, Giblin FJ, Wawrousek EF. AlphaB-crystallin in lens development and muscle integrity: a gene knockout approach. Invest Ophthalmol Vis Sci 2001;42:2924–2934. [PubMed: 11687538]

25. Bai F, Xi JH, Wawrousek EF, Fleming TP, Andley UP. Hyperproliferation and p53 status of lens epithelial cells derived from alpha B-crystallin knockout mice. J Biol Chem 2003;278:36876–36886. [PubMed: 12826669]
26. Mackay DS, Andley UP, Shiels A. Cell death triggered by a novel mutation in the alpha A-crystallin gene underlies autosomal dominant cataract linked to chromosome 21q. Eur J Hum Genet 2003;11:784–793. [PubMed: 14512969]
27. Litt M, Kramer P, LaMorticella DM, Murphey W, Lovrien EW, Weleber RG. Autosomal dominant congenital cataract associated with a missense mutation in the human alpha crystallin gene CRYAA. Hum Mol Genet 1998;7:471–474. [PubMed: 9467006]
28. Graw J, Loster J, Soewarto D, et al. Characterization of a new, dominant V124E mutation in the mouse alpha A-crystallin-encoding gene. Invest Ophthalmol Vis Sci 2001;42:2909–2915. [PubMed: 11687536]
29. Hansen L, Yao W, Eiberg H, et al. Genetic heterogeneity in microcornea-cataract: five novel mutations in CRYAA, CRYGD, and GJA8. Invest Ophthalmol Vis Sci 2007;48:3937–3944. [PubMed: 17724170]
30. Pras E, Frydman M, Levy-Nissenbaum E, et al. A nonsense mutation (W9X) in CRYAA causes autosomal recessive cataract in an inbred Jewish Persian family. Invest Ophthalmol Vis Sci 2000;41:3511–3515. [PubMed: 11006246]
31. Khan AO, Aldahmesh MA, Meyer B. Recessive congenital total cataract with microcornea and heterozygote carrier signs caused by a novel missense CRYAA mutation (R54C). Am J Ophthalmol 2007;144:949–952. [PubMed: 17937925]
32. Chang B, Hawes NL, Smith RS, Heckenlively JR, Davisson MT, Roderick TH. Chromosomal localization of a new mouse lens opacity gene (lop18). Genomics 1996;36:171–173. [PubMed: 8812430]
33. Xia CH, Liu H, Chang B, et al. Arginine 54 and Tyrosine 118 residues of alphaA-crystallin are crucial for lens formation and transparency. Invest Ophthalmol Vis Sci 2006;47:3004–3010. [PubMed: 16799046]
34. Vicart P, Caron A, Guicheney P, et al. A missense mutation in the alpha B-crystallin chaperone gene causes a desmin-related myopathy. Nat Genet 1998;20:92–95. [PubMed: 9731540]
35. Bova MP, Yaron O, Huang Q, et al. Mutation R120G in alpha B-crystallin, which is linked to a desmin-related myopathy, results in an irregular structure and defective chaperone-like function. Proc Natl Acad Sci USA 1999;96:6137–6142. [PubMed: 10339554]
36. Cobb BA, Petrash JM. Structural and functional changes in the alpha A-crystallin R116C mutant in hereditary cataracts. Biochemistry 2000;39:15791–15798. [PubMed: 11123904]
37. Shroff NP, Cherian-Shaw M, Bera S, Abraham EC. Mutation of R116C results in highly oligomerized alpha A-crystallin with modified structure and defective chaperone-like function. Biochemistry 2000;39:1420–1426. [PubMed: 10684623]
38. Hsu CD, Kymes S, Petrash JM. A transgenic mouse model for human autosomal dominant cataract. Invest Ophthalmol Vis Sci 2006;47:2036–2044. [PubMed: 16639013]
39. Liu Y, Zhang X, Luo L, et al. A novel alpha B-crystallin mutation associated with autosomal dominant congenital lamellar cataract. Invest Ophthalmol Vis Sci 2006;47:1069–1075. [PubMed: 16505043]
40. Horwitz J, Huang QL, Ding L, Bova MP. Lens alpha-crystallin: chaperone-like properties. Methods Enzymol 1998;290:365–383. [PubMed: 9534176]
41. Ho SN, Hunt HD, Horton RM, Pullen JK, Pease LR. Site-directed mutagenesis by overlap extension using the polymerase chain reaction. Gene 1989;77:51–59. [PubMed: 2744487]
42. Mach H, Middaugh CR, Lewis RV. Statistical determination of the average values of the extinction coefficients of tryptophan and tyrosine in native proteins. Anal Biochem 1992;200:74–80. [PubMed: 1595904]
43. Folta-Stogniew E, Williams KR. Determination of molecular masses of proteins in solution: implementation of an HPLC size exclusion chromatography and laser light scattering service in a core laboratory. J Biomol Tech 1999;10:51–63. [PubMed: 19499008]

44. Wen J, Arakawa T, Philo JS. Size-exclusion chromatography with on-line light-scattering, absorbance, and refractive index detectors for studying proteins and their interactions. Anal Biochem 1996;240:155–166. [PubMed: 8811899]
45. Wyatt PJ. Light scattering and the absolute characterization of macromolecules. Anal Chim Acta 1993;272:1–40.
46. Sreerama N, Woody RW. Estimation of protein secondary structure from circular dichroism spectra: comparison of CONTIN, SELCON, and CDSSTR methods with an expanded reference set. Anal Biochem 2000;287:252–260. [PubMed: 11112271]
47. Sreerama N, Woody RW. Computation and analysis of protein circular dichroism spectra. Methods Enzymol 2004;383:318–351. [PubMed: 15063656]
48. Horwitz, J. Protein Folding Handbook. Wiley-VCH Verlag GmbH; Weinheim: 2005. p. 858-875.
49. Horwitz J. Some properties of the low molecular weight alpha-crystallin from normal human lens: comparison with bovine lens. Exp Eye Res 1976;23:471–481. [PubMed: 1001375]
50. Strickland EH. Aromatic contributions to circular dichroism spectra of proteins. CRC Crit Rev Biochem 1974;2:113–175. [PubMed: 4591332]
51. Berengian AR, Bova MP, McHaourab HS. Structure and function of the conserved domain in alpha A-crystallin. Site-directed spin labeling identifies a beta-strand located near a subunit interface. Biochemistry 1997;36:9951–9957. [PubMed: 9296605]
52. Berengian AR, Parfenova M, McHaourab HS. Site-directed spin labeling study of subunit interactions in the alpha-crystallin domain of small heat-shock proteins. Comparison of the oligomer symmetry in alpha A-crystallin, HSP 27, and HSP 16.3. J Biol Chem 1999;274:6305–6314. [PubMed: 10037719]
53. Regan L. Protein structure. Born to be beta. Curr Biol 1994;4:656–658. [PubMed: 7953549]
54. de Jong WW, Caspers GJ, Leunissen JA. Genealogy of the alpha-crystallin–small heat-shock protein superfamily. Int J Biol Macromol 1998;22:151–162. [PubMed: 9650070]
55. Hejtmancik JF. Congenital cataracts and their molecular genetics. Semin Cell Dev Biol 2008;19:134–149. [PubMed: 18035564]
56. Murugesan R, Santhoshkumar P, Sharma KK. Cataract-causing alphaAG98R mutant shows substrate-dependent chaperone activity. Mol Vis 2007;13:2301–2309. [PubMed: 18199971]
57. Bera S, Abraham EC. The alpha A-crystallin R116C mutant has a higher affinity for forming heteroaggregates with alpha B-crystallin. Biochemistry 2002;41:297–305. [PubMed: 11772029]
58. Siezen RJ, Hoenders HJ. The quaternary structure of bovine alpha-crystallin. Surface probing by limited proteolysis in vitro. Eur J Biochem 1979;96:431–440. [PubMed: 572769]
59. Koteiche HA, McHaourab HS. Mechanism of a hereditary cataract phenotype. Mutations in alpha A-crystallin activate substrate binding. J Biol Chem 2006;281:14273–14279. [PubMed: 16531622]

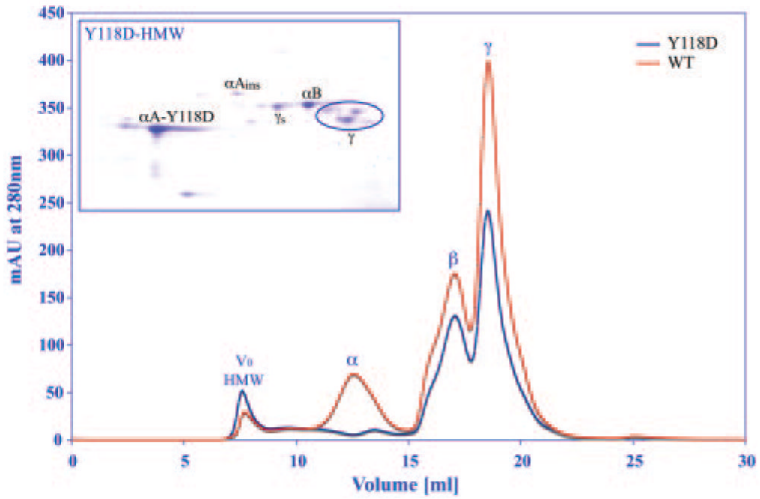

Figure 1.

Gel filtration chromatographs of total soluble proteins of wild-type (WT) and αA(Y118D/Y118D) homozygous mutant (Y118D) lenses. The peaks of high molecular weight aggregate (HMW), *α*-, *β*-, and *γ*-crystallin proteins are labeled. V_0 indicates the void volume. In the wild-type, the alpha-crystallins account for 26% of the total soluble proteins, whereas in the mutant it accounts for 12% of total soluble proteins. The 2D-gel *insert* shows a result of the HMW peak from the mutant lenses. Protein spots for αA-Y118D, αA_{insert}, αB, γ_S, and *γ*-crystallin are labeled.

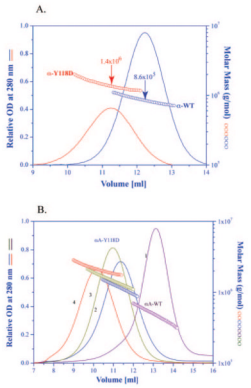

Figure 2.

(**A**) Elution profile and molar mass distribution of the α-crystallin peak obtained from a wild-type lens, and an αA(Y118D/Y118D) mutant lens shown in Figure 1. The molar mass distribution was obtained (AKTA Basic system; GE Healthcare) using a column (Superose 6 HR 10/30; GE Healthcare) connected in line with an absorption detector, a multi-angle laser light scattering detector and a refractive index detector. (**B**) Elution profile and molar mass distribution of the αA-Y118D and wild-type αA-crystallin. Curve 1, wild-type αA-crystallin at 25°C; curve 2, recombinant αA-Y118D at 25°C; curve 3, recombinant αA-Y118D after heating for 30 minutes at 37°C and then cooling back to 25°C; curve 4, recombinant αA-Y118D after heating for 30 minutes at 45°C and then cooling back to 25°C. All other conditions are the same as in Figure 1.

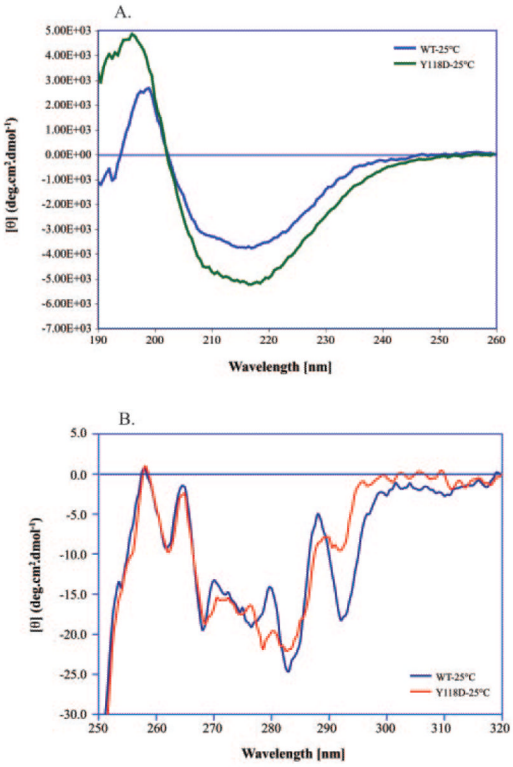

Figure 3.

Far and near ultraviolet circular dichroism spectra of recombinant wild-type αA-crystallin and recombinant αA-Y118D crystallin at 25°C. (**A**) Far ultraviolet spectra. Each spectrum represents the average of 32 scans, the pathlength was 0.2 millimeters, and the temperature was 25°C. (**B**) Near ultraviolet spectra. Each spectrum represents the average of 32 scans. The pathlength was 10 mm and the temperature was 25°C.

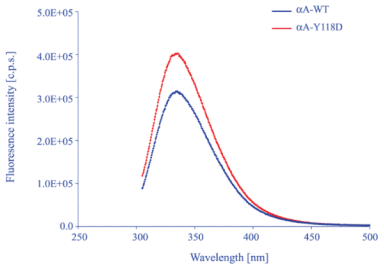

Figure 4.

Fluorescence emission spectra of recombinant wild-type αA-crystallin and recombinant αA-Y118D crystallin. Steady state fluorescence measurements were made on a spectrofluorometer (Jobin Yvon-SPEX Fluorolog τ-3; Edison, NJ); bandwidths for the excitation and emission monochromators were 2 nm and 3 nm, respectively. The excitation wavelength was set to 295 nm. Absorbances for both αA-WT and αA-Y118D recombinant proteins at 295 nm were 0.01.

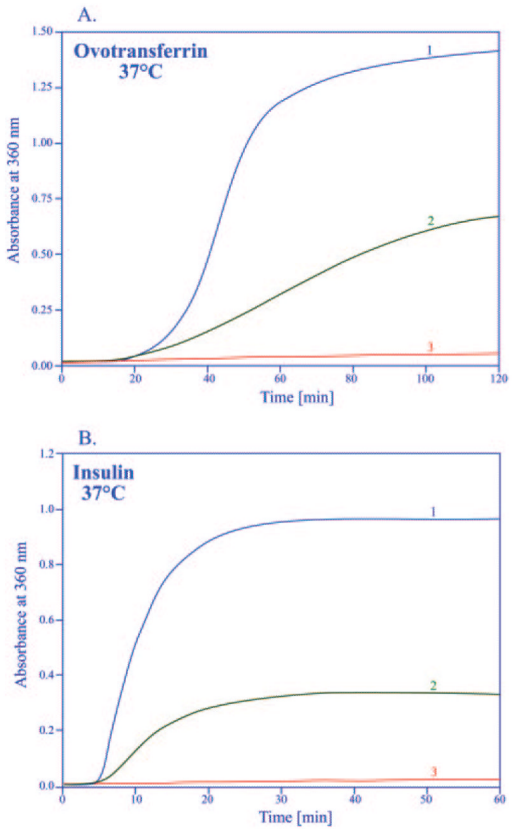

Figure 5.

Chaperone-like activity of recombinant wild-type αA-crystallin and recombinant αA-Y118D crystallin using ovotransferrin and insulin as target proteins. (**A**) Ovotransferrin: curve 1, unfolding 0.2 mg of ovotransferrin incubated with 20 mM TCEP and heated to 37°C; curve 2, same as curve 1 but with the addition of 0.4 mg of wild-type recombinant αA-crystallin; curve 3, same as curve 1 but with the addition of 0.4 mg of αA-Y118D. (**B**) Insulin: curve 1, aggregation of 0.1 mg of insulin on the addition of 5 mM TCEP at 37°C; curve 2, same as curve 1 but with the addition of 0.1 mg wild-type αA; curve 3, same as curve 1 but with the addition of 0.1 mg αA-Y118D.

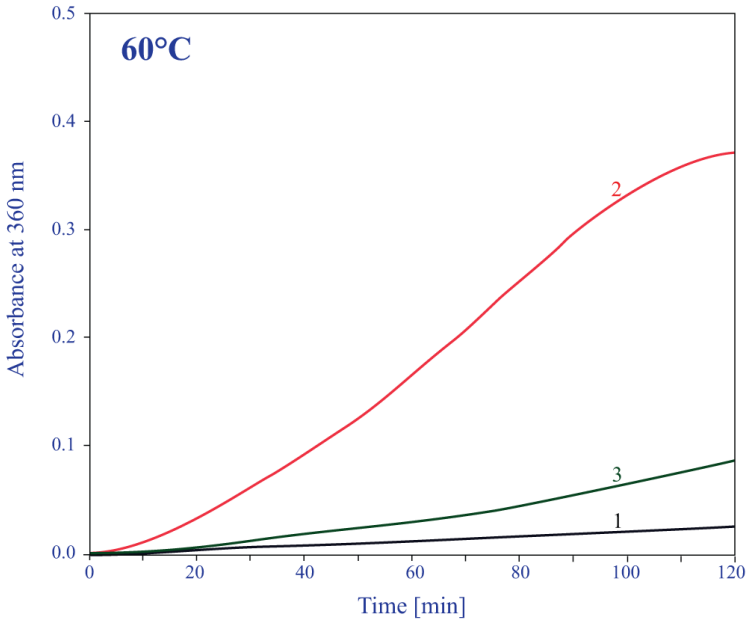

Figure 6.

Stability of total soluble lens proteins from a wild-type control mouse lens and from an αA-Y118D homozygous mouse lens at 60°C. Curve 1, 0.2 mg of total soluble protein obtained from a wild-type lens and heated to 60°C for 120 minutes in 0.5 mL; curve 2, 0.2 mg of total soluble proteins obtained from an αA-Y118D mouse lens and heated to 60°C in 0.5 mL; curve 3, same as curve 2 but with the addition of 50 microgram of recombinant αA-Y118D.

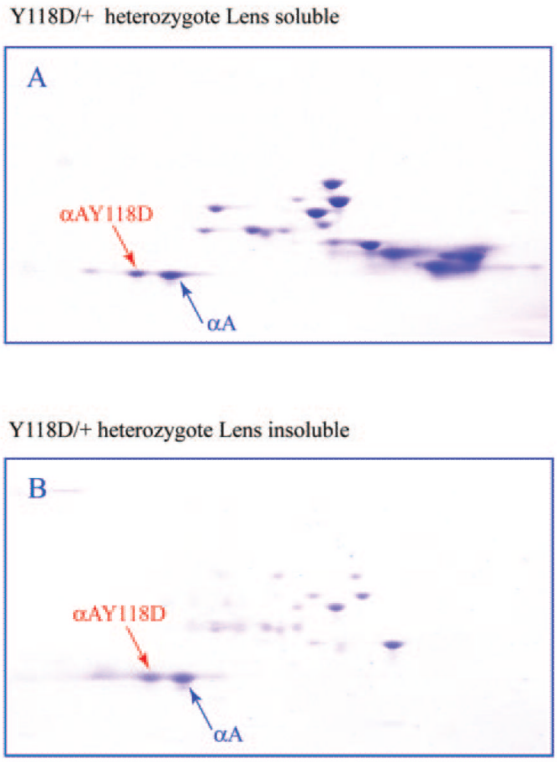

Figure 7.
Two-dimensional gel electrophoresis (2-DE) of water-soluble and water insoluble lens proteins from αA(Y118D/+) heterozygous mutant lenses. (**A**) 2-DE results of lens total water-soluble proteins (15 mg proteins were loaded). (**B**) 2-DE results of lens total water-insoluble proteins. Both wild-type αA-crystallin and mutant αA-Y118D protein spots are indicated by arrows. The pH gradient is from 3 on the *left side* to 10 on the *right side* of the 2-DE images.

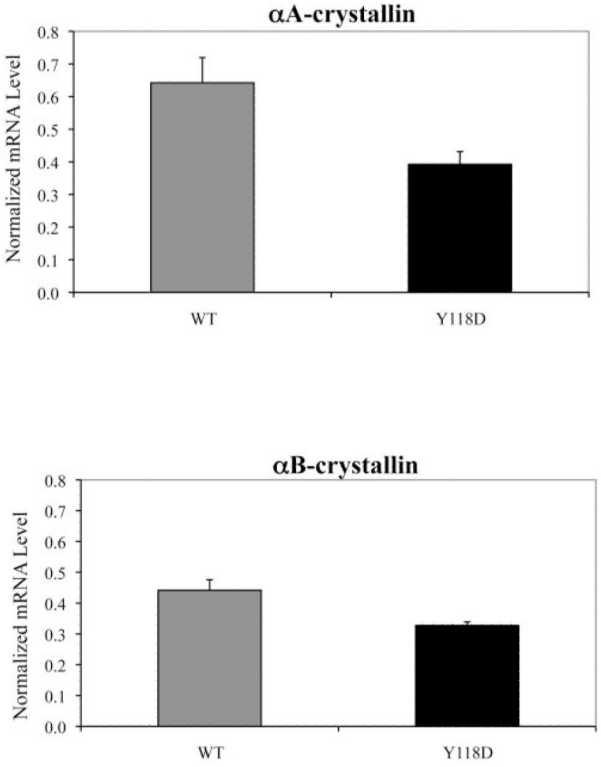

Figure 8.
Quantitative RT-PCR results of the αA- and αB-crystallin mRNA transcript levels in postnatal day 21 wild-type and αA(Y118D/Y118D) lenses.

Table 1

Far Ultraviolet Circular Dichroism Analysis of αA-WT and αA-Y118D

	α-Helix (%)			β-Sheet (%)					
Methods	**H(r)**	**H(d)**	**Total**	**S(r)**	**S(d)**	**Total**	**Turns (%)**	**Unordered (%)**	**NRMSD***
αA-WT									
CONTINLL 25°C	0.4	3.9	4.3	26.8	12.4	39.2	22.4	34.1	0.063
CONTINLL 45°C	1.8	4.6	6.4	26.7	12.4	39.1	22.6	31.9	0.031
SELCON 3 25°C	1.0	3.2	4.2	20.0	13.1	33.1	22.9	36.6	0.170
SELCON 3 45°C	1.7	5.3	7.0	27.0	14.6	41.6	22.4	26.3	0.131
CDSSTR 25°C	−0.4	4.4	4.0	27.8	13.2	41.0	24.1	29.0	0.173
CDSSTR 45°C	0.1	5.1	5.2	28.6	12.5	41.1	23.6	29.2	0.068
αA-Y118D									
CONTINLL 25°C	2.7	5.0	7.7	25.4	12.8	38.2	23.4	30.7	0.022
CONTINLL 45°C	4.2	6.4	10.6	21.6	12.4	34.0	22.2	33.1	0.029
SELCON 3 25°C	2.3	6.0	8.3	25.4	12.1	37.5	20.5	25.2	0.133
SELCON 3 45°C	4.8	7.5	12.3	22.2	11.9	34.1	20.1	31.0	0.130
CDSSTR 25°C	0.6	5.6	6.2	27.3	12.3	39.6	23.7	29.6	0.037
CDSSTR 45°C	1.6	5.1	6.7	24.3	12.1	36.4	25.2	31.3	0.119

Estimation of secondary structure parameters was performed using CDPro program CONTIN method with an expended reference set.[46,47] H(r), helix regular; H(d), helix distorted; S(r), sheet regular; S(d), sheet distorted.

*NRMSD, normalized root of mean square deviation.